[4] Visual assessment of the influence of adverse diffraction orders on the quality of image formed by the refractive-diffractive optical system

Greisukh G.I. , Ezhov E.G., Kazin S.V. , Sidyakina Z.A. , Stepanov S.A.
Penza State University of Architecture and Construction

Abstract

Adverse impact of the diffraction orders on visually assessed quality of the image formed by the refractive-diffractive optical system is investigated. It is shown that if the microstructure of diffractive lenses used in the optical system has a saw-tooth profile and brightness variations in the photographed scenes are not extreme, the adverse diffraction orders do not practically reduce the system's frequency-contrast characteristic, and the halo does not have any significant negative impact on visual perception of the image.

Keywords: *diffractive lens, relief-phase microstructure, adverse diffraction orders, image quality.*

Citation: *Greisukh G.I. Visual assessment of the influence of adverse diffraction orders on the quality of image formed by the refractive-diffractive optical system / Greisukh G.I., Ezhov E.G., Kazin S.V., Sidyakina Z.A., Stepanov S.A. // Computer Optics. – 2014. – Vol. 38(3). – P. 418-424.*

Introduction

A single diffractive lens (DL) included into an optical system consisting of refractive lenses enables (due to its unique focusing and aberration properties) to significantly simplify a system design and to obtain high optical performance at the same time. This is true both for optical systems referred to quasi-monochromatic sources of radiation [1-5] and for the systems aimed at utilization of polychromatic radiation [6-13]. In particular, when using the diffractive lens it is possible to achieve a high degree of correction of chromatic aberration required to produce high-quality color images using a limited range of optical materials such as, for example, advanced and commercially available optical plastics [14-17].

However, the diffractive mechanism of wavefront transformation on the diffractive lens microstructure, in addition to positive characteristics of optical elements of this type, poses one of the main problems significantly limiting the practical use of diffractive lenses in imaging optical systems. This problem is related to the fact that when using diffractive lenses in such systems, the leakage radiation is overlayed on the image formed by radiation diffracted on the lens microstructure to the working diffractive order which is formed due to diffraction on the same microstructure to adverse diffraction orders.

The degree and nature of adverse impact of the diffraction orders of the diffractive lens on the image quality formed by a hybrid refractive-diffractive optical system (i.e. the system containing diffractive lenses together with refractive lenses), in addition to in-order distribution of the diffraction efficiency (DE), shall depend on how much unfocused are the images formed in the adverse orders. It can be in turn determined by two factors: first, by a ratio between optical power of the diffractive lens in the working diffractive order and optical power of the whole system; second, by the spherical aberration value provided by the diffractive lens in the wavefront formed in the working diffractive order. In this paper we investigate the influence of adverse diffraction orders when both defocusing and spherical aberration is large enough, so that diameters of defocused images of a point source exceed, at least one order, the image diameter of this source formed in the working diffractive order. This is the case, in particular, when forming the image of the plastic hybrid aspheric lens (HAL) No. 5-999 manufactured by Edmund Optics for commercial purposes [18]. Therefore, researches and findings which presented herein in this paper were performed using this particular optical element.

1. Researches and findings

The hybrid aspheric lens whose optical layout is shown in Fig. 1 has been manufactured from Zeonex E48R optical plastic and has got aspheric and spherical refracting surfaces.

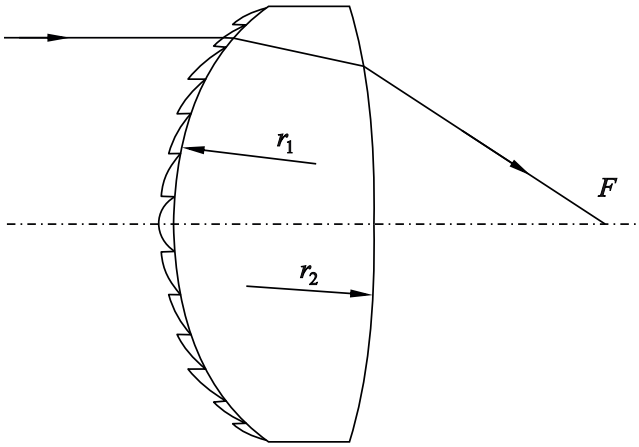

Fig. 1. Optical layout of the Plastic Hybrid Aspheric Lens No 65-999: radius of curvature at the peak of the aspheric surface $r_1 = 12.5$ mm, radius of the aspheric surface $r_2 = -48.3$ mm; axial thickness $d = 3.3$ mm; clear aperture $D = 10$ mm

A sawtooth relief-phase diffraction microstructure of the diffractive lens is provided, as shown in Fig. 1, by the aspheric surface. Phase delay caused by the diffractive lens microstructure in the wavefront ψ and its focal length f'_{DL} are described, respectively, by the following equations [19]

$$\psi = mA_1\rho^2, \tag{1}$$

$$f'_{\mathrm{DL}} = -\pi/mA_1\lambda. \tag{2}$$

In these equations m – is a number of the diffractive order, ρ – is a length measured relative to the optical axis, and the coefficient $A_1 = -16.411$ mm^{-2}.

The effective focal length of the hybrid aspherical lens in wavelength of the helium yellow d–line ($\lambda_{\mathrm{d}} = 0.58756$ μm) is $f' = 18.025$ mm, and the focal length of the hybrid aspheric lens in the +1st working diffractive order is $f'_{\mathrm{DL}} = 325.8$ mm. The spherical aberration of the hybrid aspheric lens has been completely eliminated (not exceeding 0.001λ) in wavelength λ_{d} for the axial point source taken at infinity from the diffractive lens. The depth of the sawtooth relief of the diffractive lens microstructure has been selected with reference to condition of the maximum diffraction efficiency close to 100%, particularly, at this wavelength. The microstructure within limits of the clear aperture includes 65 Fresnel zones. We should point out here that with regard to the sawtooth relief-phase microstructure of the diffractive lens the term "Fresnel zone" means a microstructure area, within limits of which the phase delay caused by the microstructure in the wavefront incident on it shall vary from 0 to 2π [1, 20]. The width of any of the above 65 Fresnel zones shall be not less than $\Lambda_{\min} = 40$ μm, whereas the relief depth determined in accordance with formula [1]

$$h = \lambda_{\mathrm{d}}/(n_{\mathrm{d}} - 1) \tag{3}$$

is $h = 1.106$ μm, since the refraction index for Zeonex E48R plastic in wavelength λ_{d} is $n_{\mathrm{d}} = 1.5311$ [21]. If we have the above number of Fresnel zones and if $\Lambda_{\min}/h > 36$, the actual diffraction efficiency, which may be estimated by numerical solutions of Maxwell's equations, is practically in line with the assessment obtained within the framework of the scalar diffraction theory and in approximation of infinitely thin transparent [22, 23]. Therefore, in order to estimate the diffraction efficiency in different diffractive orders we will use below the equation obtained in the scalar approximation and reduced, for example, in [22]:

$$\eta_m = \left\{ \frac{\sin\left[\pi\left(\Delta l/\lambda - m\right)\right]}{\pi\left(\Delta l/\lambda - m\right)} \right\}^2 \tag{4}$$

where λ – is the wavelength of the structure-incident light, Δl – is an increment of the optical distance in one period of the sawtooth profile, and in our case $\Delta l = h(n-1)$, and n – is the plastic material refraction index on the wavelength λ.

The hybrid aspheric lens is achromatized for a visual spectral band limited with blue F– and red C– lines of hydrogen ($\lambda_{\min} = \lambda_{\mathrm{F}} = 0.48613$ μm and $\lambda_{\max} = \lambda_{\mathrm{C}} = 0.65626$ μm). Therefore, the table below gives the values of diffraction efficiency for a number of diffractive orders particularly on these wavelengths. At the same time, the values of diffraction efficiency are also given on the He-Ne laser wavelength ($\lambda_{\mathrm{HeNe}} = 0.6328$ μm), on which researches were also performed. Diffractive orders higher than the 5th order have not been included into the table and were not taken into consideration in the analysis, since their energy impact is negligibly small.

Table. Distribution of diffractive efficiency of the saw-tooth relief-phase microstructure in accordance with diffractive orders on three wavelengths

No. of diffractive order, m	Diffractive efficiency on wavelength $\lambda = \lambda_F$	$\lambda = \lambda_{HeNe}$	$\lambda = \lambda_C$
+1	0.8457	0.9817	0.9612
0	0.02828	0.006436	0.0145
-1	0.00857	0.001486	0.00322
+2	0.07032	0.00477	0.00935
-2	0.004076	0.000644	0.00138
+3	0.0134	0.00128	0.0026
-3	0.002374	0.000358	0.00076
+4	0.0055	0.000582	0.0019
-4	0.00155	0.000227	0.00048
+5	0.00297	0.000332	0.000682
-5	0.00109	0.000157	0.000345

For separate monitoring of images of infinitely remote point source formed by the hybrid aspheric lens in different diffractive orders, a circular peripheral lens area of diameter 1.5 mm was illuminated with a parallel and normally incident beam of He-Ne laser. The picture on how the peripheral area of the diffractive lens operates in various diffractive orders is schematically shown in Fig. 2. The photo of a pilot unit assembled on a "SYN"-type interferometer table is shown in Fig. 3, and the picture recorded with a video camera and reproduced on a monitor's screen is shown in Fig. 4.

We herewith note that simultaneous recording, using a matrix image sensor, of the images the brightness of which differ from each other by many orders, can be achieved due to their spatial separation and appropriate selection of the intensity of the beam incident on the hybrid aspheric lens. As a result, pixels perceiving unfocused images of high orders can operate in linear mode, and pixels perceiving the focused image of the first order can operate in saturation mode.

The image defocusing grows in accordance with the growing number of both positive and negative diffractive orders, since an increment magnitude of the effective focal length of the hybrid aspheric lens also grows with the number growing.

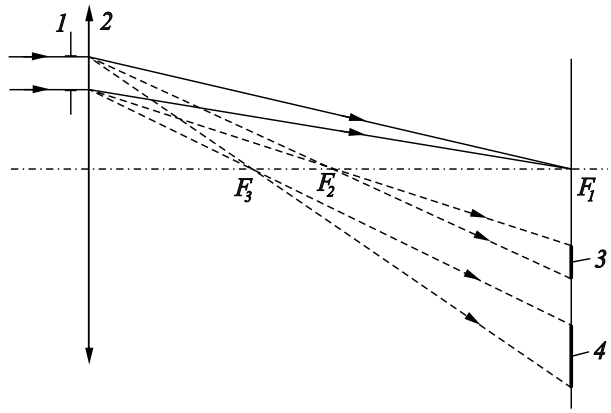

Fig.2. Layout of formation and displacement of defocused images in the +1st, +2nd and +3rd diffractive orders: 1– is an off-axis aperture diaphragm; 2-is the diffractive lens: F1-F3 – are back focuses of the diffractive lens in proper diffractive orders; 3, 4 – are defocused images formed in the +2nd and +3rd diffraction orders

Fig. 3. Pilot unit assembled on the "SYN"-type interferometer table and enabled to transfer the formed picture to computer for analysis

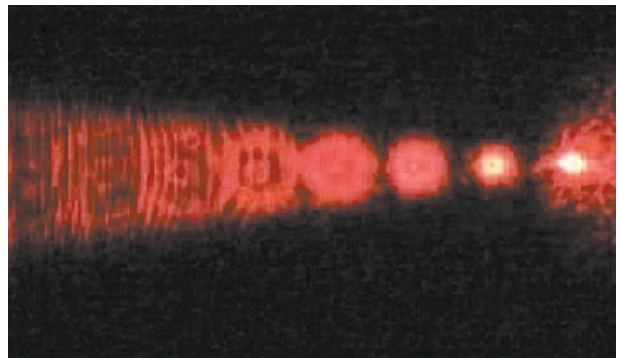

Fig. 4. Images of the infinitely remote point source formed by the hybrid aspheric lens in eight (from m =+8 to m =+1) diffraction orders (number of orders decreases from left to right); the image contrast is inverted in accordance with printing requirements

The picture shown in Fig. 4 fits well to the beam scattering pattern formed by Zemax optical design software [24] and shown in Fig. 5.

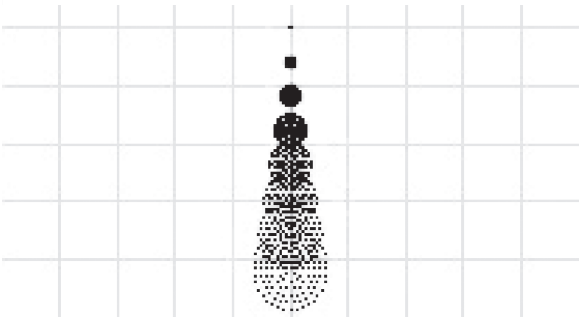

Fig. 5. Beam scattering diagram built by Zemax optical software

Quality evaluation of the image of an extended object formed by the hybrid aspheric lens was performed in accordance with the frequency-contrast characteristic being computed by Zemax software, as well as experimentally using a test target. A line target developed and manufactured by "Svetlana" Joint Stock Company (RF), a leading microelectronic and electronic devices manufacturing company, was used as the test target. It is very similar to the world-widely used Resoluting Power Test Target USAF 1951 [25] (see Fig. 6), but it is reduced, if compared with the original, so that the number of line pairs per one millimeter is 100 times greater in the zeroth group than in the original. As a result, the number of line pairs per one millimeter in any three-tie element of the used line target is determined by the equation

$$N_{G;E} = 100 \cdot 2^{[G+(E-1)/6]} \qquad (5)$$

where G – is the number of a group of elements (in Fig. 6 G possesses the value of 0 and 1), and E – is the number of the element (in Fig. 6 E varies from 1 to 6).

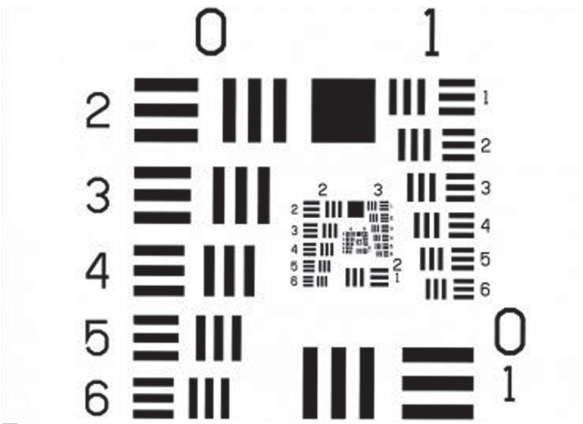

Fig. 6. Resoluting Power Test Target USAF 1951 including ties of the 0th and 1st groups with elements from 1 to 6

The line target was installed perpendicularly to the optical axis of the hybrid aspheric lens from the side of the spherical surface and its center was set on the optical axis, and the length between the test target and the frontal area of the hybrid aspheric lens, i.e. a front section was selected closely to the effective focal length of the hybrid aspheric lens: $s = -18.3$ mm. It provided a linear increase $\beta = -8.81$ acceptable for image analysis in the process of spherical aberration on the wavelength λ_d in plane of the best unit for this wavelength not exceeding 0.05λ. The line target was lighted with an electric filament lamp (coil temperature was 3200 K) through UV&IR Cut Filter [26] with a spectral bandpass from λ =0.42 μm to λ =0.68 μm. As a result, the relative radiation intensity on the line target was within the range from 0.17 (on the wave length λ =0.42 μm) to 1.0 (on the wavelength λ =0.68 μm). On the wavelengths on which the hybrid aspheric lens was approximated the relative intensity amounted to 0.38 (on λ_F) and 0.95 (on $\lambda_{\tilde{N}}$).

In the line target image formed by the hybrid aspheric lens on a CCD matrix and observed on monitor screen (see Fig. 7), the ties of the element 6 in group 0 are well resolved. In accordance with formula (5) the spatial frequency of the first harmonic in this element is $N_{0;6}$ =178 lin/mm (the width of the ties and the length between them is 2.81 μm).

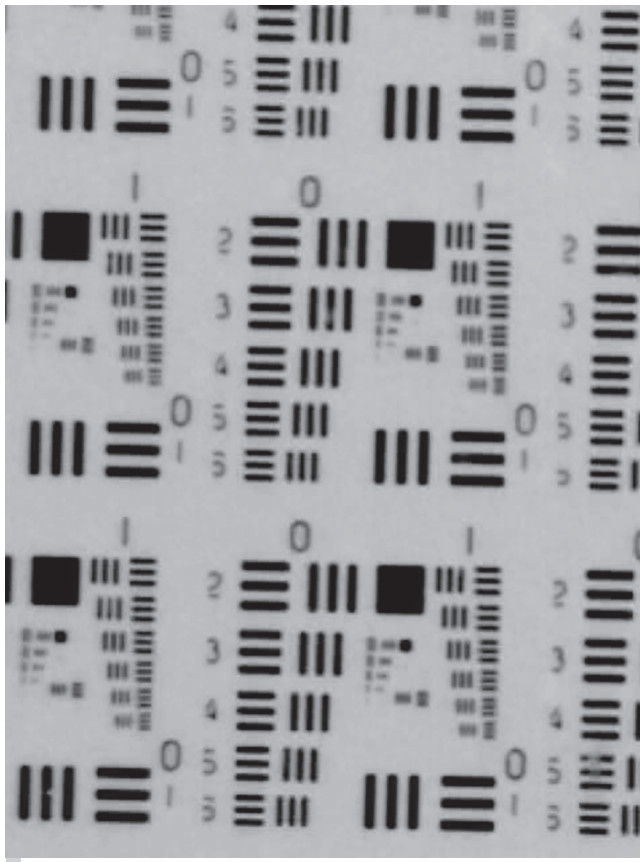

Fig. 7. Image of the line target manufactured by Svetlana JSC produced by the hybrid aspheric lens registered with the video camera and displayed on monitor screen; the image contrast is inverted in accordance with printing requirements

The ties of the element 1 in group 1 are less well resolved. The spatial frequency of the first harmonic in this element is $N_{1;1}$ =200 lin/mm (the width of the ties and the length between them is 2.5 μm). In the image plane all dimensions are $|\beta|$ =8.81 times more and the frequencies are the same times less, whereas 20.2 lin/mm corresponds to the frequency $N_{ù}$, and 22.7 lin/mm – to the frequency $N_{1;1}$.

We should note here that the resolution, both in the image transferred by the CCD matrix to the computer and in the image observed on monitor screen, is completely determined by the hybrid aspheric lens, since the resolution power of the CCD matrix and computer's monitor exceeds, at least by one order, the tie passing frequency in a proper image of the line target.

The polychromatic frequency-contrast characteristic computed by Zemax software for spatial frequencies of 20 and 23 lin/mm with respect to only the $+1^{st}$ working diffraction order gives contrast values of 0.28 and 0.24, respectively. The polychromatic frequency-contrast characteristic which takes into account all diffraction orders (up to $m = \pm 5$) gives practically indistinct contrast values. This owes to the fact that in view of the measurable optical power of the diffractive lens being a part of the hybrid aspheric lens, the images formed in adverse diffraction orders seemed to be so much defocused that in combination with the low diffraction efficiency in these orders they create a very weak and almost uniform background having practically no effect on the contrast of the focused image formed in the working diffraction order. This conclusion is confirmed by the quality of the image shown in Fig. 6, as well as by good coincidence of rated and experimentally obtained contrasts.

Referring again to Fig. 6 we should note that a light-field square element of the line target enables to evaluate the galo influence stipulated by availability of adverse diffraction orders, on the visual perception of the image formed by the hybrid aspheric lens. There is no galo in the image shown in Fig. 7. In order to determine conditions for its occurrence the lighting intensity of the line target was increased. This lighting intensity was brought up to the level at which the contrast was considerably reduced in the line target image due to the fact that the radiation passing through its chromium slab considerably exceeded a threshold of sensitivity of the CCD matrix. However, even in this case no halo could be observed. It can be discovered if we replace the line target with an opaque screen supplied with a small-sized hole. If compare the hole images formed by the hybrid aspheric lens and a single refractive lens with the comparable focal length and the clear aperture, it can be concluded that appearance of the halo was caused whether by light scattering on optical element rims or by light diffraction to adverse diffraction orders of the diffractive lens.

Conclusion

Experimental results submitted in the present paper have demonstrated the visual perception to be conformed to the rated quality evaluation of the polychromatic image formed by the investigated refractive-diffractive optical system. Wherein the galo stipulated by the light diffracted to adverse diffraction orders of the diffractive lens may adversely affect the perception of scene images with only high brightness variations, which usually overlap the frequency range of area imagers in mobile phones and CCTV videocameras. Therefore, the adverse dif-

fraction orders of the sawtooth relief-phase structure are not considered to be an obstacle to use the diffractive lens in such devices.

Acknowledgements

This work has been performed with the financial support of the Ministry of Education and Science of the Russian Federation within the framework of the state task in the field of university research activities.

References

1. Bobrov, S.T Optics of diffractive elements and systems / S.T. Bobrov, G.I. Greisukh, Yu.G. Turkevich. – L.: Mashinostroenie. – 1986. – P. 223. (In Russian).

2. Greisukh, G.I. Optics of diffractive and gradient-index elements and systems [Text] / G. I. Greisukh, S. T. Bobrov, S. A. Stepanov. – Bellingham: SPIE Press. – 1997. – P. 414.

3. Greisukh, G.I. Optical systems with diffractive elements: ways of the chromatism correction / G.I. Greisukh, E.G. Ezhov, S.V. Kazin, S.A. Stepanov // Computer Optics. – 2010. – Vol. 34(2). – P. 187-193. (In Russian).

4. Greisukh, G.I. Design of the double-telecentric high-aperture diffractive–refractive objectives / G.I. Greisukh, E.G. Ezhov, I.A. Levin, S.A. Stepanov // Applied Optics. – 2011. – Vol. 50(19). – P. 3254-3258.

5. Greisukh, G.I. Potentialities of achromatized diffractive and diffractive-refractive X-ray focusing systems / G.I. Greisukh, E.G. Ezhov, S.V. Kasin, S.A. Stepanov // Technical Physics. – 2012. – Vol. 57(3). – P.410-414.

6. Gan, M.A. Theory and design methods of the hologram and kinoform optical elements / M.A. Gan. – L: GOI. – 1984. – P. 140. (In Russian).

7. Mercado, R.I. The design of apochromatic optical systems / R.I. Mercado // International Lens Design Conference, SPIE. – 1985. – Vol. 554. – P. 217-227.

8. Stone, T. Hybrid diffractive-refractive lenses and achromats / T. Stone, N. George // Applied Optics. – 1988. – Vol. 27. – P. 2960-2971.

9. Maxwell, J. Tertiary spectrum manipulation in apochromats / J. Maxwell // International Lens Design Conference, SPIE. – 1990. – Vol. 1354. – P. 408-411.

10. Mercado, R.I. Designs of two-glass apochromats and superachromats / R.I. Mercado // International Lens Design Conference, SPIE. – 1990. – Vol. 1354. – P. 263-272.

11. Greisukh, G.I. Diffractive-Refractive Hybrid Corrector for Achro– and Apochromatic Corrections of Optical Systems / G.I. Greisukh, E.G. Ezhov, S.A. Stepanov // Applied Optics. – 2006. – Vol. 45(24). – P. 6137-6141.

12. Greisukh, G.I. Diffraction-refraction corrector of the tertiary spectrum / G.I. Greisukh, E.G. Ezhov, S.V. Kasin, S.A. Stepanov // Journal of Optical Technology. – 2010. – Vol. 77(9). – P. 542-547.

13. Greisukh, G.I. Modeling and investigation superachromatozation refractive and refractive-diffractive optical systems / G.I. Greisukh, E.G. Ezhov, I.A. Levin, A.V. Kalashnikov, S.A. Stepanov // Computer Optics. – 2012. – Vol. 36 (3). – P. 395-404. (In Russian).

14. Greisukh, G.I. Design of achromatic and apochromatic plastic microobjectives / G.I. Greisukh, E.G. Ezhov, I.A. Levin, S.A. Stepanov // Applied Optics. – 2010. – Vol. 49(23). – P. 4379-4384.

15. Greisukh, G.I. Diffractive–refractive correction units for plastic compact zoom lenses / G.I. Greisukh, E.G. Ezhov, A.V. Kalashnikov, S.A. Stepanov // Applied Optics. – 2012. – Vol. 51(20). – P. 4597-4604.

16. Greisukh, G.I. Design of plastic diffractive–refractive compact zoom lenses for visible–near-IR spectrum / G.I. Greisukh, E.G. Ezhov, Z.A. Sidyakina, S.A. Stepanov // Applied Optics. – 2013. – Vol. 52(23). – P. 5843-5850.

17. Greisukh, G.I. Design and analysis of the compact plastic refractive-diffractive zoom lens / G.I. Greisukh, E.G. Ezhov, Z.A. Sidyakina, S.A. Stepanov // Computer Optics. – 2013. – Vol. 37(2). – P. 210-214. (In Russian).

18. Edmund Optics: plastic hybrid aspheric lenses [Electronic resource]. – Access mode: http://www.edmundoptics.com/optics/optical-lenses/aspheric-lenses/plastic-hybrid-aspheric-lenses/3200

19. Geary, J.M. Introduction to lens design: with practical ZEMAX examples / J.M. Geary. – Richmond: Willmann-Bell, Inc. – 2002. – P. 462.

20. Koronkevich, V.P. Modern zone plates / V.P. Koronkevich, I.G. Palchikova / Autometrija. – 1992. – Vol.1. – P. 85-100. (In Russian).

21. Optical Component and Lens Applications [Electronic resource]. – Access mode: http://www.zeonex.com/optical_plastic.asp

22. Greisukh, G.I. Suppression of the Spectral Selectivity of Two-Layer Relief-Phase Diffraction Structures / G.I. Greisukh, E.A. Bezus, D.A. Bykov, E.G. Ezhov, S.A. Stepanov // Optics and Spectroscopy. – 2009. – Vol. 106(4). – P. 692-697.

23. Greisukh, G.I. The efficiency of relief-phase diffractive elements at a small number of Fresnel zones / G.I. Greisukh, E.G. Ezhov, A.V. Kalashnikov, I.A. Levin, S.A. Stepanov // Optics and Spectroscopy. – 2012. – Vol. 113(4). – P. 425-430.

24. ZEMAX: software for optical system design [Electronic resource]. – Access mode: http://www.radiantzemax.com

25. 1951 USAF resolution test chart [Electronic resource]. – Access mode: http://en.wikipedia.org/wiki/1951_USAF_resolution_test_chart

26. HOYA FILTERS [Electronic resource]. – Access mode: http://www.hoyafilter.com/hoya/products/generalfilters/uvircut. – 1991. – P. 1232. (In Russian).